Host-Specific Transcriptional Responses of *Phytophthora capsici* During Early Crown Infection in Cucurbitaceous and Solanaceous Plants

Pablo Vargas-Mejía[1,2,3], Lino Sánchez Segura[4], Fernando U. Rojas-Rojas[1,2,], Harumi Shimada-Beltrán[1,2] and Julio C. Vega-Arreguín[1,2*]

[1]Laboratorio de Ciencias AgroGenómicas, Escuela Nacional de Estudios Superiores Unidad León, UNAM, Blvd. UNAM 2011, 37684, León, México.

[2]Laboratorio Nacional PlanTECC, Escuela Nacional de Estudios Superiores Unidad León, UNAM, Blvd. UNAM 2011, 37684, León, México.

[3]Posgrado en Ciencias Biológicas, Universidad Nacional Autónoma de México, CDMX, México.

[4]Centro de Investigación y de Estudios Avanzados del Instituto Politécnico Nacional. Unidad Irapuato, Km. 9.6, Libramiento Norte, Carretera Irapuato-León, Guanajuato, 36824, México.

***Corresponding author:** JCVA (jvega@enes.unam.mx)

Keywords: RNA-seq; *Phytophthora capsici*; Host-pathogen interactions; Effector regulation; Metabolic reprogramming; Oomycete pathogenesis; Virulence strategies; Generalist pathogen

Abstract

Phytophthora capsici is a broad-host-range oomycete phytopathogen responsible for economic losses in crops worldwide. Previous transcriptomic analyses have focused mainly on plant responses to infection. However, the transcriptional adaptations of the phytopathogen to different host species remain poorly understood. In this study, we investigated the transcriptomic response of *P. capsici* during early infection in *Cucumis sativus, Cucumis melo, Capsicum annuum* CM334, and *Solanum lycopersicum* by RNA-seq and multiphoton microscopy. Focusing on crown infections since it is the natural entry point for the pathogen.

Our results reveal striking host-specific infection strategies. In tomato, rapid necrosis at 12-27 hours post-inoculation was associated with early metabolic reprogramming and effector repression. In contrast, cucurbits exhibited delayed necrosis (36-102 hpi), supporting extensive

host intracellular colonization and upregulation of carbohydrate metabolism pathways. Partially resistant CM334 chili pepper restricted pathogen proliferation, with *P. capsici* displaying transcriptional signatures indicative of metabolic stress. In addition, effector expression is tightly regulated, with the differential deployment of RxLR, NLP, and CRN families across hosts.

Comparative transcriptomics highlights metabolic reprogramming as a key determinant of infection success, with *P. capsici* fine-tuning its gene expression to exploit host-specific vulnerabilities. These findings provide novel insights into *P. capsici* adaptive strategies in soil-borne infections and underscore the importance of targeting crown infection sites for disease management. Future research should integrate host transcriptomics and functional studies to elucidate the molecular determinants of host specificity.

1 Introduction

Phytophthora capsici is a notorious filamentous phytopathogenic oomycete responsible for severe symptoms in vegetable, ornamental, and tropical crops, such as root and stem rot, lower size in plants, and necrosis (Quesada-Ocampo et al., 2023). These symptoms produce a yield decrease and, in severe cases, loss of crops around the world. (Lamour et al., 2012b). As a soil-borne pathogen with a broad host range, *P. capsici* infects several species of *Cucurbitaceae* and *Solanaceae* families, causing the first symptoms of diseases in the root, such as root rot and subsequent stem blight and fruit rot. *P. capsici* displays adaptative strategies to colonize its hosts, and it is considered a generalist phytopathogen; it has a highly adaptable infection strategy, allowing it to overcome diverse plant defense mechanisms (Quesada-Ocampo et al., 2023). Despite its significance, our understanding of the molecular mechanisms underlying host-specific infection strategies remains incomplete. Most of the previous studies have been focused on plant transcriptomic responses to *P. capsici*, and fewer have investigated how the pathogen modulates its gene expression in response to different hosts and infection niches giving valuable insights into pathogen adaptation and virulence (Chen et al., 2013; Jupe et al., 2013; Maillot et al., 2022). Besides, most transcriptomic studies of *P. capsici* were focused on foliar infection, even though this pathogen naturally enters plants mostly through soil and colonize roots and the crown region (Hausbeck and Lamour, 2004). The crown infection niche presents unique physiological and immunological features in terms of its structural characteristics, nutrient availability, and the

63 composition of host defense mechanisms that may influence pathogen gene expression and
64 virulence strategies (Knight and Sutherland, 2016; Stephens et al., 2008).
65
66
67 The early infection stage is particularly critical, as *P. capsici* must rapidly establish and grow
68 within host tissues while evading recognition by host immune receptors. Pathogen success during
69 this phase depends on the precise regulation of effector proteins, metabolic reprogramming, and
70 stress adaptation mechanisms (Judelson, 2017; Wang et al., 2023; Zuluaga et al., 2016). Notably,
71 effector proteins such as RxLRs and Crinklers (CRNs) play essential roles in suppressing plant
72 immune responses, while secreted hydrolytic enzymes facilitate tissue colonization (Chepsergon
73 et al., n.d.; Stam et al., 2021; Wang et al., 2023; Zuluaga et al., 2016). On the other hand, metabolic
74 plasticity also plays a key role, as *P. capsici* must exploit host-derived nutrients while resisting
75 oxidative stress imposed by plant defenses (Judelson, 2017).
76
77 Despite these advances, the host-dependent transcriptomic responses of *P. capsici* remain poorly
78 characterized, particularly in the context of crown infections in multiple hosts. Comparative
79 transcriptomics of the pathogen across different plant species can reveal core virulence
80 determinants as well as host-specific adaptations that shape infection outcomes. Understanding
81 how *P. capsici* fine-tunes its gene expression in response to diverse host environments is crucial
82 for developing targeted disease management strategies.
83
84 The aim of this study was to elucidate the transcriptomic responses of *P. capsici* during infection
85 of four host species: two cucurbitaceous hosts (cucumber and melon) and two solanaceous hosts
86 (CM334 chili pepper and tomato). Notably, our experimental design focused on infections initiated
87 at the crown of the plant, rather than the more commonly examined foliar infections. This approach
88 is particularly relevant given that *P. capsici* is a soil-borne pathogen that exploits the crown region
89 to establish systemic colonization. By investigating the transcriptomic profiles of *P. capsici* in
90 these hosts at the early infection stage, we aimed to provide insights into the molecular
91 determinants of host-specific virulence, as well as the metabolic adaptations that facilitate
92 successful colonization.
93

2 Materials and methods

2.1 Strains, Media and Culture Conditions

The *Phytophthora capsici* strain used in this study was D3 mating type A1 (Pons-Hernández et al., 2020; Sevillano-Serrano et al., 2024). *P. capsici* D3 was routinely grown on V8 agar in the dark at 24°C.

2.2 Infection Assay

To infect seedlings with *P. capsici* D3, 0.01 g of mycelium from 5 days-old cultures was harvested with tweezers and deposited in the crown of 5-8 weeks-old seedlings. Plants used as hosts in the present study were *Capsicum annuum* (Criollo de Morelos 334), *Cucumis melo*, *Cucumis sativus*, and *Solanum lycopersicum*. As a non-plant infection control, the same mycelium source was cultivated on V8 agar plates. At 24 hours post-inoculation, the accessible mycelium on the infected plant surface was recovered with tweezers for subsequent RNA extraction.

2.3 Multiphoton microscopy

Stems and roots were dissected from a 1 cm distance to the crown inoculation site. Samples were fixed in 4% paraformaldehyde and incubated during 2 h. Subsequently, the samples were washed with phosphate buffer 0.16 M at pH 7.2 and embedded in Sakura Tissue Tek, and frozen at -20°C. The samples were sectioned in a cryotome to a width of 100 µm. Tissue sections were stained with Propidium Iodine (IP) at a final concentration of 0.0003%. To stain the cell wall, the samples were treated with Solophenyl at 0.01%. The stained samples were visualized in multiphoton microscopy LSM 880-NLO Axio Imager Z2 microscope (Zeiss, Oberkochen, Germany) coupled to a Ti:Sapphire infrared laser (Chameleon Vision II, COHERENT, Santa Clara, CA, USA). The excitation laser was set at 543 nm for Propidium iodine and 458 nm for Solophenyl, respectively. The emission was detected from 548 to 684 for IP and 502 to 558 nm for Solophenyl. All micrographs were captured in CZI format at 1131 × 1131 pixels and RGB color. The spectral graphs were analyzed in Sigma plot 12 (Systat Software, Inc.).

2.4 RNA Extraction and Illumina Sequencing

Total RNA was extracted using the Quick-RNA Plant Miniprep Kit (Zymo Research, CA, USA) according to manufacturer's protocol, omitting the Zymo-Spin III-HRC column in the final step.

Mycelia of 10 infected plants were pooled per extraction, and 0.1g of mycelia was used for each extraction. RNA quality was measured with a Bioanalyzer, and samples with RIN > 5 were used for sequencing. RNA-Seq libraries (15 libraries in total, representing five conditions with three biological replicates per condition) were prepared by selectively isolating mRNA using poly-T oligo-attached magnetic beads. Libraries were sequenced at Novogene (Sacramento, CA, USA) using the Illumina NovaSeq 6000 platform (Hayward, CA, USA), generating paired-end reads (2 × 150 bp) with an average yield of 50 million reads per library. The raw sequencing data have been deposited in the NCBI database under BioProject accession number PRJNA1207595.

2.5 Mapping and statistical analysis

Read trimming and adaptor removal were performed using BBDuk with the parameters `forcetrimleft=20` and `trimq=20` (https://sourceforge.net/projects/bbmap/). Mapping and quantification were conducted with Kallisto using the *P. capsici* LT1534 v11.0 transcriptome (available at MycoCosm: mycocosm.jgi.doe.gov) (Bray et al., 2016; Grigoriev et al., 2014; Lamour et al., 2012a), employing bias correction and 100 bootstrap replicates. Approximately 77% of reads were pseudoaligned to the transcriptome. Differential expression analysis was carried out using DESeq2, as described in (Love et al., 2014; Tanja, 2023). *P. capsici* grown on V8 agar served as the control condition. Transcripts with an adjusted p-value (p-adj) ≤ 0.05 and a log2FoldChange > 1 or < -1 were considered differentially expressed genes (DEGs). Co-expression analysis was executed with Clust 1.18, using the parameters `-no optimization` (Abu-Jamous and Kelly, 2018).

2.6 Functional enrichment

In order to identify Gene Ontology (GO) terms and KEGG pathway enrichment, the reference transcriptome was re-annotated using eggNOG mapper v2.1.12 (Huerta-Cepas et al., 2019) and merged with existing MycoCosm annotations. Effector proteins, including RXLRs, CRNs, Elicitins, and Nep1-like proteins (NLPs), were retrieved from the literature and supplemented by identifying additional candidates using EffectorP v3.0. Additional secreted proteins were predicted using SignalP v6 (Sperschneider and Dodds, 2022; Teufel et al., 2022). Functional enrichment analysis was performed with clusterProfiler v4.12.6, employing an over-representation analysis

155 (ORA) approach and applying a *p*-value cutoff of ≤0.05 (Wu et al., 2021). Effectors were annotated
156 against various databases with BLAST using an evalue < $1x10^{-30}$.
157
158 **2.7 Functional validation by RNAi**
159 Functional validation by gene silencing of three effector genes was conducted by designing RNAi
160 sequences and their respective primers using SIREN v0.1.5
161 (https://github.com/pablovargasmejia/SIREN), and the T7 promoter was added to each primer
162 (Table S1). To avoid off-targets in the pathogen and host plants, an off-target database was
163 constructed with the cDNA sequences of *P. capsici* and the four host plants with the --targets option
164 in SIREN v0.1.5. Designed RNAi sequences were *in vitro* transcribed from *P. capsici* cDNA fused
165 with the T7 promoter using HighYield T7 RNAi Kit at 37°C for 4 h (Jena Bioscience, Germany).
166 RNAi experiments were performed as follows: 1 µg of synthetic dsRNA were incubated with 0.1
167 g of *P. capsici* mycelium for 2 h on ice to facilitate cellular uptake. Then, 0.01 g of treated
168 mycelium was used as inoculum for virulence assays on adult plant leaves or plantlet stems. As a
169 negative control for silencing, *P. capsici* mycelium was incubated as described with T7 reaction
170 components that excluded RNA production. To screen the disease phenotype of the silenced genes,
171 inoculated leaves and stems were cleared first in an acetic acid: ethanol (1:3, v/v) solution
172 overnight, then in an acetic acid: ethanol: glycerol (1:5:1, v/v/v) solution for 3 h. The samples were
173 subsequently incubated for 3 h in a staining solution of 0.01% (w/v) trypan blue and then stored
174 in 60% glycerol until examination.
175
176 **3 Results**
177 **3.1 Host Susceptibility and Stem Colonization**
178 To evaluate host susceptibility to *P. capsici* D3, we infected the crown of *C. annuum* (Criollo de
179 Morelos 334 chili pepper), *C. melo* (melon), *C. sativus* (cucumber), and *S. lycopersicum* (tomato)
180 plantlets with mycelia. Representative phenotypes of 5-8 weeks plants at 24 hours post inoculation
181 (hpi) are shown in Figure 1a-d. Among the tested hosts, cucumber exhibited the most pronounced
182 aerial mycelial growth (Figure 1a-d), followed by melon, and subsequently by chili pepper and
183 tomato. Interestingly, the extent of mycelial growth on the surface of the infected tissue was
184 contrary to the time required for the pathogen to induce necrosis in the cucumber melon and tomato
185 plants (Figure 1e).

186 Tomato was the most susceptible host; the first symptoms of necrosis were observed at 12 hpi for
187 some individuals, and the median time for infected plants to show necrosis was 27 hpi, reflecting
188 a rapid progression of the infection. In contrast, the cucurbitaceous hosts displayed symptoms of
189 necrosis at later times post-inoculation. Melon plants started to show necrosis at 36 hpi, with the
190 median time of symptom appearance in melon plants population at 54 hpi, while cucumber plants
191 began to necrose at 48 hpi, reaching a median necrosis onset at 102 hpi. Notably, chili pepper
192 (CM334), a genotype previously reported to be partially resistant to *P. capsici* infection, exhibited
193 an even further delayed necrotic response, with first symptoms evident at 90 hpi and a median
194 necrosis onset at 120 hpi (Figure 1e).
195
196 Despite the delayed necrosis induction, in cucurbitaceous plants, greater intercellular mycelial
197 growth was observed in these hosts during the sampled period. At 24 hpi, stem cross-sections
198 dissected from 1 cm above the inoculation area showed abundant intercellular *P. capsici* D3
199 mycelial growth particularly in vascular tissues and in apoplastic manner (Figure 1f, g; Figure S1).
200 In the tissue, the solophenyl (channel green) and propidium iodide staining (channel red) stained
201 cell walls of the plants and mycelium of *P. capsici* D3 respectively.
202
203 Tomato plants showed large mycelial growth. Contrary to the cucurbitaceous plants, the pathogen
204 grew longitudinally into parenchyma tissue, surrounding but not invading the vascular tissue
205 (Figure 1i). Interestingly, chili pepper plants did not show intercellular mycelial growth in stem
206 tissues at 24hpi (Figure 1h). Further examination of the inoculation site, and 1cm distal stems at
207 48 hpi confirmed that *P. capsici* D3 could not penetrate or invade chili pepper tissues effectively
208 at these time points prior to necrosis (Figure S2).
209
210 **3.2 Tissue-Specific Infection Dynamics: Root and Stem**
211 To evaluate the tissue-specific pattern infection, we examined intercellular mycelium growth in
212 the roots of infected melon, and chili pepper seedlings. At 24 hpi, *P. capsici* exhibited low
213 proliferation in the roots of melon and at 48 hpi pathogen showed a small increase in root
214 colonization (Figure 2a). This could suggest that the pathogen showed more affinity to stems rather
215 than roots (Figure 1f-i and 2c-d).

Consistent with observations at the stem, mycelial growth was not detectable in chili pepper roots even when the pathogen developed appressorium at 24 and 48 hpi (Figure 2b and S3). At 96 hpi, infection progression showed *P. capsici* mycelial growth extending into the aerial photosynthetic parts of tomato, at 120 hpi in melon and cucumber, and at 144hpi in pepper chili plantlets. This observation suggests that *P. capsici* tends to colonize the aerial portions of its hosts, despite initial zoospore deposition being concentrated at the crown, roots, and stem base under field conditions (Figure S4).

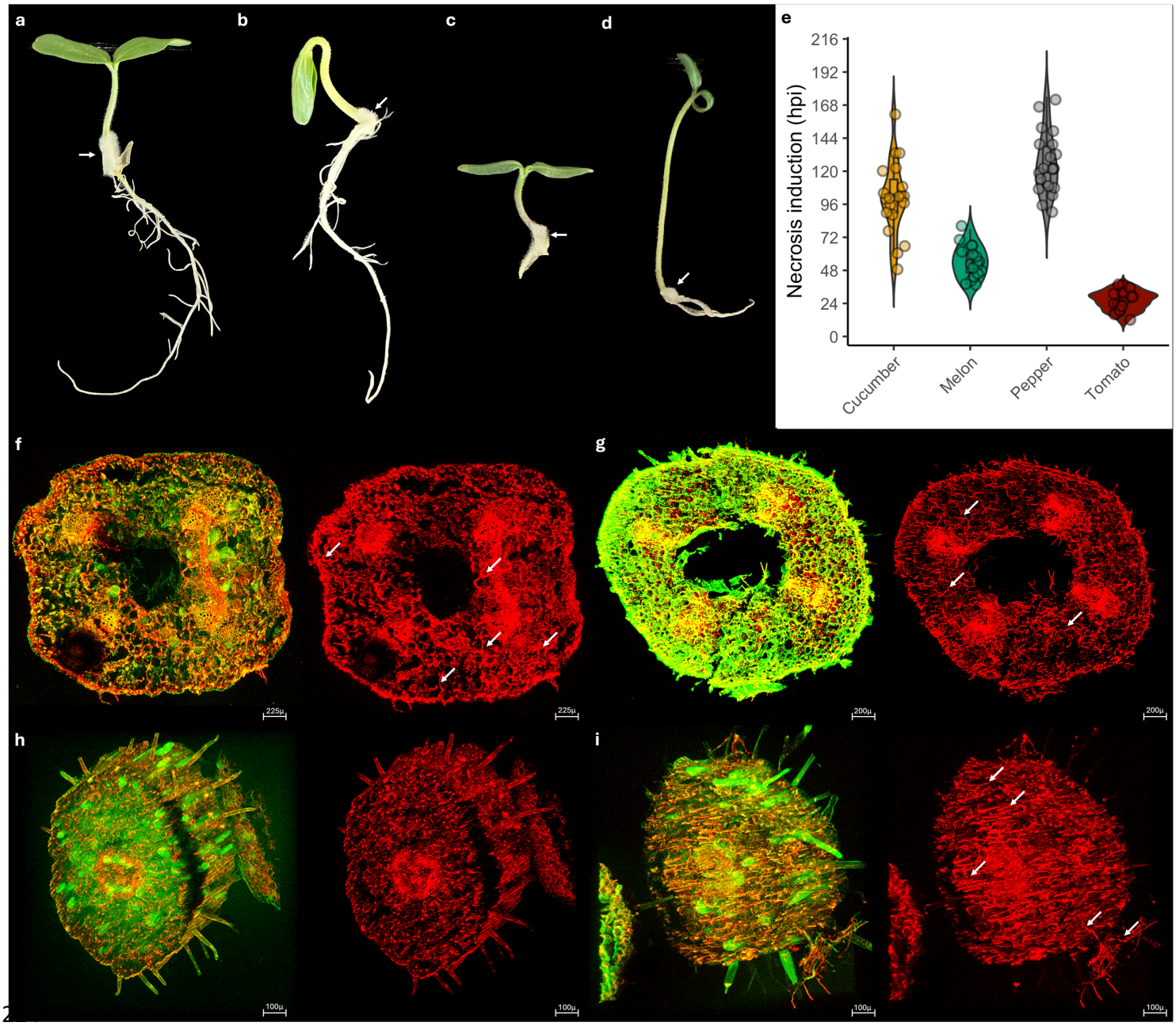

Figure 1: Dynamics of *P. capsici* infection. **a** Cucumber (24 hpi). **b** Melon (24 hpi). **c** Chili pepper (24 hpi). **d** Tomato (24 hpi). **e** Time to necrosis induction by the host. **f** Stem section of cucumber infected plant at 24 hpi **g** Stem section of melon infected with *P. capsici* at 24 hpi. **h** Chili pepper stem section infected (24 hpi). **i** Stem section of tomato infected with *P. capsici* (24 hpi). White arrows highlight portions of mycelium. The plant cell wall was stained with solophenyl flavine

(green channel) and the hyphae of *P. capsici* was stained with propidium iodide (red channel). For each host left image presents both channels, right image only presents propidium iodine staining.

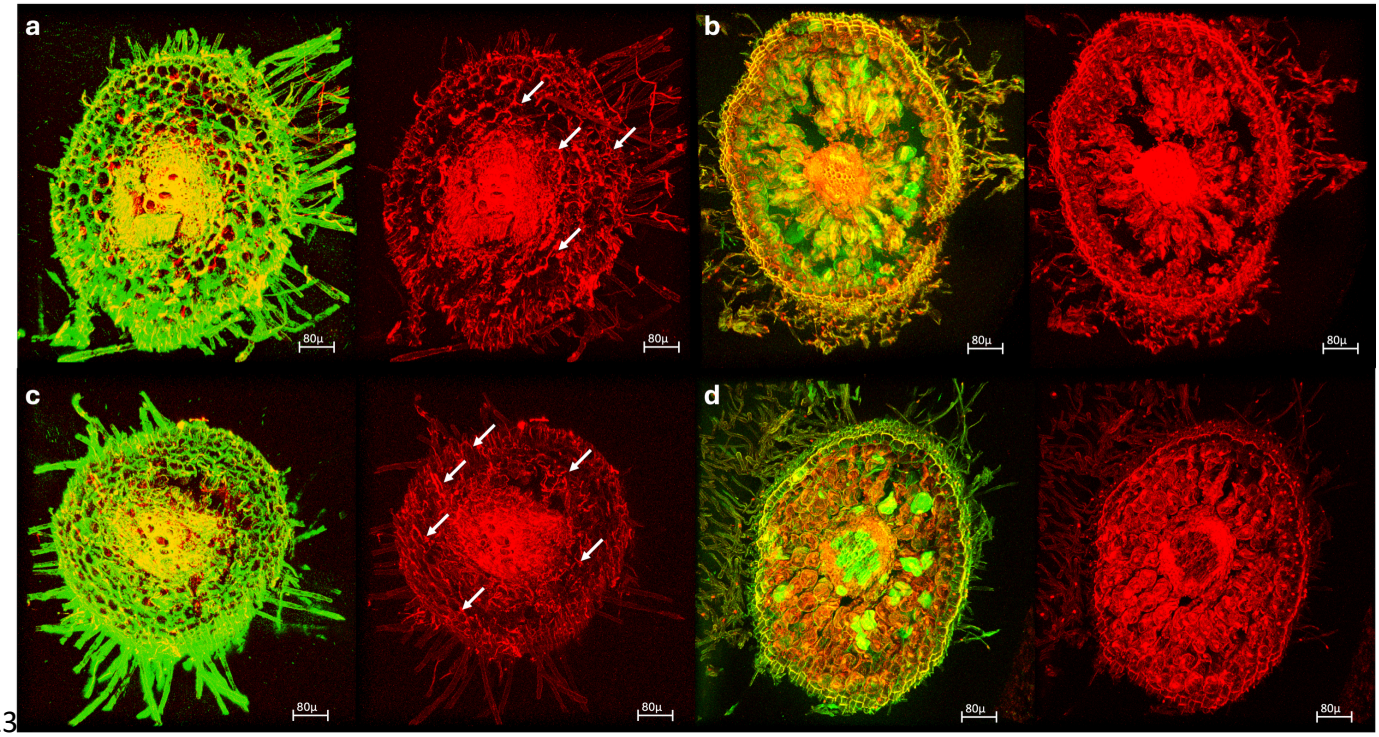

Figure 2: Root colonization of *P. capsici*. **a** Melon root at 24 hpi. **b** Chili pepper root at 24hpi. **c** Melon root at 48 hpi. **d** Chili pepper root at 48 hpi. White arrows highlight portions of mycelium. The plant cell wall was stained with solophenyl flavine (green channel) and the hyphae of *P. capsici* was stained with propidium iodide (red channel). For each host left image presents both channels, right image only presents propidium iodine staining.

3.3 Comparative Transcriptomic Analysis Reveals Host-Dependent Pathogenic Strategies

We decided to perform RNA-Seq of *P. capsici* infecting the Solanaceous and Cucurbitaceous hosts to understand the transcriptional response of the pathogen to the diverse environments that each host represents. Mapping to the reference transcriptome yielded an average mapping rate of 77% for each library. After principal component analysis, we found an evident separation of the transcriptome responses of the *Phytophthora* samples when the pathogen was infecting a host compared to the pathogen growing in V8 agar media (Figure 3a). Also, PCA showed an aggrupation of the transcriptomic responses for the cucurbits and tomato infections, although 1 tomato sample was grouped with the chili pepper samples (Figure 3a).

248

Table 1: Differentially expressed genes*

Condition	Total genes	Up regulated	Down regulated
Cucumber	2270	1281	989
Melon	2366	1167	1199
Chili pepper	2872	1268	1604
Tomato	2104	1104	1000
Total Unique	4470	2226	2307

249 *padj < 0.05 Log2FC > 1 OR < -1

250

251 Of the 19805 transcripts of *P. capsici*, 4470 genes were found as differentially expressed (DEGs =
252 padj < 0.05 and Log2FC > 1 OR < -1) among all conditions when compared to our control of
253 pathogen growing in V8 media (Table 1). We found on average around 2300 DEGs for each
254 sample, being the tomato infections where less differentially expressed genes were observed, and
255 chili pepper the condition with the most differentially expressed genes (Table 1). Of the 4470
256 DEGs we found that only 436 were induced among all conditions and 415 were down-regulated,
257 indicating that the core transcriptome of *P. capsici* infecting four different hosts is not composed
258 of a large number of genes (Figure 3b, c). This core set of DEGs shared across all *P. capsici*
259 infection conditions was subjected to Gene Ontology (GO) and KEGG pathway enrichment
260 analysis to uncover key biological processes and pathways involved in the plant-pathogen
261 interaction. Between biological processes, significant enrichment was observed for processes
262 associated with metabolic activity, including fatty acid metabolism, carbohydrate metabolic
263 processes, and glycolysis, alongside defense-related processes such as pathogenesis and electron
264 transport (Figure S5a). Additionally, terms related to cell wall modification and phosphate
265 transport were prominent, reflecting the infection and nutrient acquisition by the pathogen.

266

267 Pathway enrichment analysis showed a diverse range of metabolic pathways (Figure S5b). These
268 included fatty acid beta-oxidation, glycolysis/gluconeogenesis, and amino acid metabolism,
269 suggesting a reconfiguration of primary metabolic networks during infection. Notably, pathways
270 associated with mobilization of nutrients from the host, such as glycerolipid and galactose
271 metabolism, were upregulated emphasizing the pathogen's strategy to exploit host resources. In

272 parallel, the enrichment of pathways related to defense mechanisms, including alkaloid
273 biosynthesis and gamma-hexachlorocyclohexane degradation, underscores the activation of plant
274 immune responses. The differential enrichment of these pathways in upregulated and
275 downregulated DEGs provides insights into the dynamic interplay between metabolic
276 reprogramming and adaptation to host defense during *P. capsici* infection.
277
278 The transcriptional response of *P. capsici* revealed a remarkable adaptability to the unique micro
279 ecological niches generated by its hosts. While some processes were shared, the pathogen's
280 specific enrichments varied considerably, reflecting its ability to exploit host-specific
281 vulnerabilities and overcome distinct physiological and defense barriers.
282
283 In solanaceous hosts, particularly tomato, *P. capsici* prioritized pathways associated with rapid
284 energy acquisition, such as glycolysis and fatty acid metabolism. This metabolic change was
285 probably evidenced by the faster strategy of colonization of the pathogen, which corresponds to
286 the host's early necrotic response. Interestingly, during tomato infection, *P. capsici* also showed
287 enrichment of alkaloid degradation pathways, suggesting that the pathogen may counteract host-
288 produced antimicrobial compounds, including alkaloids to establish infection. The capacity of *P.*
289 *capsici* to degrade these compounds evidences the intense chemical warfare between tomato and
290 *P. capsici*, with the pathogen leveraging its metabolic flexibility to neutralize host defenses (Figure
291 3d, e).
292
293 In contrast, infection of the partially resistant chili pepper CM334 exhibited a distinct pattern of
294 transcriptional enrichment in the pathogen (Figure 3). Processes related to cell wall modification
295 and lipid metabolism were notably upregulated in *P. capsici* during its attempted colonization of
296 chili pepper. These enrichments, including pathways such as terpenoid and glycerolipid
297 metabolism, suggest that *P. capsici* was preparing to breach structural barriers and colonize the
298 host. However, the absence of detectable pathogen growth within chili pepper tissues at 24hpi
299 (Figure 1c and h) implies that the mechanism of infection was insufficient to overcome the physical
300 and biochemical defenses of this plant. Additionally, the enrichment of nitrogen compound
301 metabolism pathways in *P. capsici* during chili pepper infection may indicate an effort to adapt to
302 nutrient scarcity, reflecting a limitation imposed by the host resistance mechanisms.

303

304 In cucurbitaceous hosts (melon and cucumber), *P. capsici* shifted its transcriptional priorities
305 toward metabolic reprogramming to exploit the nutrient-rich environment provided by these hosts
306 (Figure 3d, e). Melon infection was characterized by strong enrichment in carbohydrate
307 metabolism, including galactose and glycerolipid pathways, and processes like nitrogen utilization
308 and protein glycosylation (Figure 3d, e). These adaptations showed the capacity of the pathogen
309 to use the host abundant resources to support its growth and effector production. Similarly, in
310 cucumber, *P. capsici* exhibited significant enrichment in glycolysis and gluconeogenesis,
311 suggesting an intensified focus on extracting energy and carbon from the host. The pathways
312 related to transport, such as phosphate and copper transport, were also highly enriched in
313 cucurbitaceous hosts.

314

315 The stark differences in enrichment between partially resistant chili pepper CM334 and the more
316 susceptible cucurbitaceous hosts emphasize the dynamic nature of the *P. capsici* infection
317 strategies. In chili pepper, the pathogen appears to invest heavily in preparatory mechanisms to
318 overcome structural and chemical defenses, albeit unsuccessfully in this case. Conversely, in more
319 susceptible hosts, *P. capsici* capitalizes on the availability of nutrients and the relative lack of
320 effective defensive barriers to drive its infection forward. These findings illustrate how *P. capsici*
321 tailors its transcriptional profile to exploit or confront the unique challenges posed by each host.

322

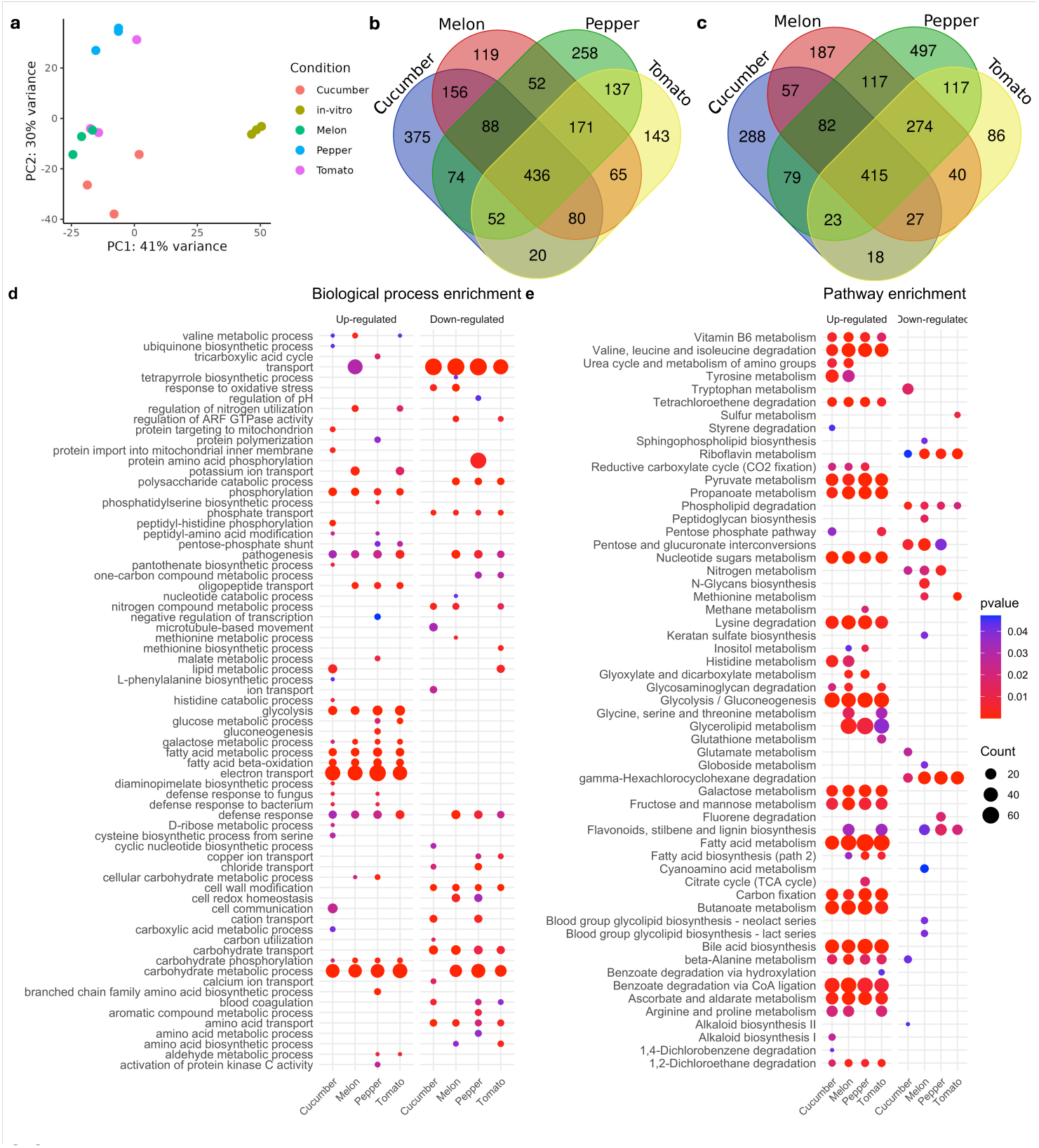
a
PC2: 30% variance
PC1: 41% variance
Condition
Cucumber
in-vitro
Melon
Pepper
Tomato
b
Cucumber
Melon
Pepper
Tomato
119
258
156
52
137
375
88
171
143
74
436
65
52
80
20
c
Cucumber
Melon
Pepper
Tomato
187
497
57
117
117
288
82
274
86
79
415
40
23
27
18
d
Biological process enrichment
Up-regulated
Down-regulated
valine metabolic process
ubiquinone biosynthetic process
tricarboxylic acid cycle
transport
tetrapyrrole biosynthetic process
response to oxidative stress
regulation of pH
regulation of nitrogen utilization
regulation of ARF GTPase activity
protein targeting to mitochondrion
protein polymerization
protein import into mitochondrial inner membrane
protein amino acid phosphorylation
potassium ion transport
polysaccharide catabolic process
phosphorylation
phosphatidylserine biosynthetic process
phosphate transport
peptidyl-histidine phosphorylation
peptidyl-amino acid modification
pentose-phosphate shunt
pathogenesis
pantothenate biosynthetic process
one-carbon compound metabolic process
oligopeptide transport
nucleotide catabolic process
nitrogen compound metabolic process
negative regulation of transcription
microtubule-based movement
methionine metabolic process
methionine biosynthetic process
malate metabolic process
lipid metabolic process
L-phenylalanine biosynthetic process
ion transport
histidine catabolic process
glycolysis
glucose metabolic process
gluconeogenesis
galactose metabolic process
fatty acid metabolic process
fatty acid beta-oxidation
electron transport
diaminopimelate biosynthetic process
defense response to fungus
defense response to bacterium
defense response
D-ribose metabolic process
cysteine biosynthetic process from serine
cyclic nucleotide biosynthetic process
copper ion transport
chloride transport
cellular carbohydrate metabolic process
cell wall modification
cell redox homeostasis
cell communication
cation transport
carboxylic acid metabolic process
carbon utilization
carbohydrate transport
carbohydrate phosphorylation
carbohydrate metabolic process
calcium ion transport
branched chain family amino acid biosynthetic process
blood coagulation
aromatic compound metabolic process
amino acid transport
amino acid metabolic process
amino acid biosynthetic process
aldehyde metabolic process
activation of protein kinase C activity
Cucumber
Melon
Pepper
Tomato
e
Pathway enrichment
Up-regulated
Down-regulated
Vitamin B6 metabolism
Valine, leucine and isoleucine degradation
Urea cycle and metabolism of amino groups
Tyrosine metabolism
Tryptophan metabolism
Tetrachloroethene degradation
Sulfur metabolism
Styrene degradation
Sphingophospholipid biosynthesis
Riboflavin metabolism
Reductive carboxylate cycle (CO2 fixation)
Pyruvate metabolism
Propanoate metabolism
Phospholipid degradation
Peptidoglycan biosynthesis
Pentose phosphate pathway
Pentose and glucuronate interconversions
Nucleotide sugars metabolism
Nitrogen metabolism
N-Glycans biosynthesis
Methionine metabolism
Methane metabolism
Lysine degradation
Keratan sulfate biosynthesis
Inositol metabolism
Histidine metabolism
Glyoxylate and dicarboxylate metabolism
Glycosaminoglycan degradation
Glycolysis / Gluconeogenesis
Glycine, serine and threonine metabolism
Glycerolipid metabolism
Glutathione metabolism
Glutamate metabolism
Globoside metabolism
gamma-Hexachlorocyclohexane degradation
Galactose metabolism
Fructose and mannose metabolism
Fluorene degradation
Flavonoids, stilbene and lignin biosynthesis
Fatty acid metabolism
Fatty acid biosynthesis (path 2)
Cyanoamino acid metabolism
Citrate cycle (TCA cycle)
Carbon fixation
Butanoate metabolism
Blood group glycolipid biosynthesis - neolact series
Blood group glycolipid biosynthesis - lact series
Bile acid biosynthesis
beta-Alanine metabolism
Benzoate degradation via hydroxylation
Benzoate degradation via CoA ligation
Ascorbate and aldarate metabolism
Arginine and proline metabolism
Alkaloid biosynthesis II
Alkaloid biosynthesis I
1,4-Dichlorobenzene degradation
1,2-Dichloroethane degradation
Cucumber
Melon
Pepper
Tomato
pvalue
0.04
0.03
0.02
0.01
Count
20
40
60

Figure 3: Transcriptional responses of *P. capsici* to different hosts. **a** Principal component analysis of *P. capsici* transcript expression. **b** Venn diagram of up-regulated DEGs. **c** Venn diagram of down-regulated DEGs. **d** Biological process and **e** KEGG Pathway enrichment of *P. capsici* differentially expressed genes.

3.4 Host-Dependent Effector Expression Profiles

We found a total of 70 RxLRs, 28 Elicitins, 18 CRNs, and 17 NLPs effectors differentially expressed. RxLR expression was mainly down-regulated except for 12 genes, and its expression was grouped according to the family of the infected host; the same behavior was found for the CRN effectors (Figure 4). However, Elicitins showed a clustering for melon, tomato, and chili pepper, out-grouping cucumber condition as the most different. NLPs expression showed a clustering for tomato, cucumber, and melon, with chili pepper as the most dissimilar condition for this effector family expression. NLPs were also mainly repressed, with just 5 NLPs overexpressed. A review of the annotated RxLR effectors in our dataset reveals a diverse arsenal with distinct expression patterns that align with previously reported functions. For example, several instances homolog to PsAvh328 (genes Pc123179, Pc128001, and Pc552887) have been shown in earlier studies to interfere with host defense signaling and modulate immune responses (Wang et al., 2011). Interestingly, while some Avh328 homologs remain unexpressed under some conditions, gene Pc123179 is induced in chili pepper, suggesting a specialized role in overcoming host-specific defenses. Similarly, PsAvh16 (Pc14944, Pc14948, and Pc533084) has been implicated in suppressing programmed cell death, thereby aiding the pathogen in establishing a biotrophic interaction (Fedkenheuer, 2016). Gene Pc13391, which encodes for the uncharacterized Avh166, consistently shows downregulation across all hosts, possibly indicating its involvement at earlier/later infection stages or under environmental cues not captured in our current sampling. Pc20942 showed marked downregulation across conditions may reflect a tightly regulated deployment. The effector PcAvh103 (gene Pc536383), has been linked to the manipulation of EDS1 thus facilitating virulence, however, in our data was downregulated at all hosts infections (Li et al., 2020).

Our expression analysis of elicitin-encoding genes in *P. capsici* reveals notable variability across host conditions. Several elicitins including genes Pc16186, Pc21853, and Pc127268 exhibit robust positive expression in all hosts. However, gene Pc508761 (annotated as INF2B) is strongly

355 repressed in melon and tomato, and gene Pc508770 (INF1-like) is not induced in cucumber, chili
356 pepper, and tomato, but exhibits moderate repression in melon. INF1 is one of the best-
357 characterized elicitins, known in *P. infestans* for its sterol-binding activity and its ability to elicit
358 a hypersensitive response in a range of plant hosts (Ah-Fong et al., 2021; Du et al., 2017). Also,
359 INF2B is related to triggering HR (Huitema et al., 2005). The observed repression of both INF1
360 and INF2B in melon and for INF2B also in tomato suggests that *P. capsici* may actively
361 downregulate these elicitors to avoid triggering host defense responses and avoid necrosis during
362 its biotrophic stage.
363
364 Crinkler (CRN) effectors form a large and diverse family in oomycetes that can manipulate host
365 cell death and immune responses. In our dataset, the CRN125 homolog (gene Pc131973) is
366 strongly expressed in cucumber and melon but is downregulated in chili pepper and not induced
367 in tomato, hinting at a role tailored to the cucurbit host environment as proposed to interact with
368 cucurbit TCP14-1 or TCP14-2 to enhance virulence (Stam et al., 2021). Multiple entries annotated
369 as CRN15 show variable patterns: for example, gene Pc50894 is expressed in both cucumber and
370 melon but not in the other hosts, while gene Pc106668 also annotated as CRN15 is upregulated in
371 melon, chili pepper, and tomato. In contrast, CRN10 (gene Pc506739) is expressed solely in
372 cucumber, and CRN10 homologs (genes Pc109378 and Pc80099) are downregulated in chili
373 pepper and tomato, suggesting distinct regulatory controls even among closely related CRNs.
374 Other CRN annotations, such as CRN77 (gene Pc128631) and CRN34 (gene Pc117855), exhibit
375 modest expression in specific hosts (CRN77 in cucumber and melon, and CRN34 prominently in
376 melon) whereas members like CRN5 (gene Pc540976) and CRN21 (gene Pc133238) show little
377 to non-expression, possibly reflecting functions that are restricted to particular infection stages or
378 conditions. Pc559084 was induced in all hosts, this gene was shown to be able to suppress HR
379 triggered by INF1 but increase disease susceptibility on *N. benthamiana* plants (Chen et al., 2015).
380 Many CRNs in *P. capsici* remain uncharacterized. The diverse expression profiles observed here
381 underscore the potential for functional specialization within the CRN family and highlight the need
382 for further research to unravel their roles in host-specific pathogenicity.
383
384 Nep1-like proteins (NLPs) are a diverse family of secreted effectors known to induce necrosis in
385 dicotyledonous plants by binding to membrane glycosylinositol phosphorylceramides (GIPCs)

(Lenarčič et al., 2017). In our dataset, the expression profiles of several NLPs reveal distinct, host-dependent regulation. For example, gene Pc9358 annotated as PcNLP14 is uniquely induced in chili pepper while remaining unexpressed in cucumber, melon, and tomato. PcNLP14 was previously shown to be one of the most expressed NLP effectors in chili pepper and *N. benthamiana* and its agroinfiltration in plants showed induction of necrosis (Feng et al., 2014). In contrast, gene Pc122048 shows moderate induction in both cucumber and melon but is absent in chili pepper and tomato. Similarly, gene Pc129784 PcNLP2 another inductor of necrosis is induced in cucumber exclusively, further supporting host-specific functions among NLPs (Chen et al., 2018). On the other hand, several NLPs including gene Pc107869 and its close homolog gene Pc108964 are consistently repressed in melon, chili pepper, and tomato indicating that their expression could be tightly controlled to avoid premature host cell death (Chen et al., 2018). Other NLPs, such as gene Pc108039 NLP4 and gene Pc119748 NLP6, exhibit strong repression specifically in chili pepper and melon, whereas genes Pc18373 and Pc69122 are broadly downregulated across all hosts.

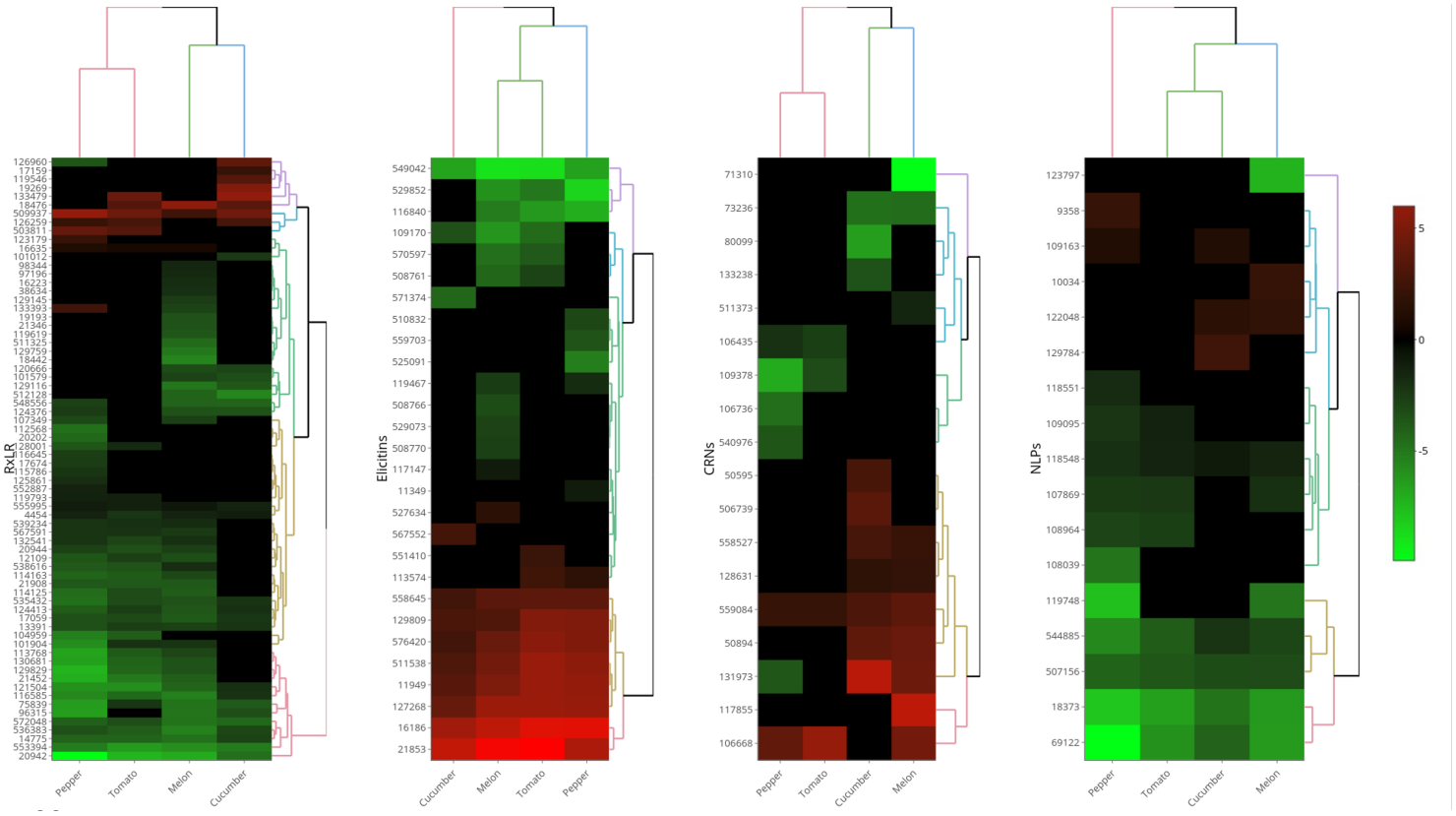

Figure 4: Heatmap of differentially expressed *Phytophthora* RxLR, elicitin, CRN, and NLP effectors

403 **3.5 Host and Tissue-Specific Phenotypes Associated with Effector Gene Silencing**

404 We investigated the role of four *P. capsici* genes by silencing via direct incubation with dsRNA.
405 Targeted genes included the differentially expressed necrosis- and ethylene-inducing peptide-like
406 protein (NLP Pc9358), induced exclusively in chili pepper; the RxLR effector Pc503811, induced
407 in chili pepper and tomato; the RxLR effector Pc18476, induced across all susceptible hosts
408 (cucumber, melon, and tomato) (Figure 4); and a non-differentially expressed conserved cell-cycle
409 gene (Pc533030, encoding SDA1), known to be essential for sporangial morphology, mycelial
410 growth, and virulence (Zhu et al., 2016). Pathogen mycelia were incubated with corresponding
411 dsRNAs for 2 h prior to infection assays on detached leaves and plantlet stems, near to the crown
412 to better mimic the conditions from previous experiments.

413 After 96 hpi control *P. capsici* showed growth on detached cucumber leaves. In contrast, all
414 dsRNA treatments exhibited a decrease in pathogen growth: Pc503811 (18.24%), Pc9358
415 (65.29%), PcSDA1 (76.47%), and Pc18476 (78.82%) (Figure 5a). For tomato detached leaves,
416 measured at 72 hpi, PcSDA1 dsRNA treatment unexpectedly showed a 10.58% increase in
417 pathogen growth, whereas Pc503811 and Pc9358 treatments reduced growth by 76.51% and
418 84.6%, respectively (Figure 5b–c).

419 In plantlet stem infections (96 hpi), cucumber showed no differences between dsRNA treatments
420 and control (Figure 5d). Similarly, melon stems infected with dsRNA-treated pathogen exhibited
421 pathogen growth comparable to control, although dsRNA treatments notably prevented the
422 appearance of necrosis. Conversely, in chili pepper and tomato stems, the PcSDA1 dsRNA-treated
423 pathogen induced aggressive necrosis, surpassing control severity and causing complete tissue
424 necrosis. In chili pepper, Pc18476 and Pc503811 dsRNA treatments resulted in reduced pathogen
425 growth by 54% and 68%, respectively, yet failed to prevent necrosis. Notably, Pc9358 dsRNA
426 treatment, while causing a more moderate 32% growth reduction, completely prevented necrosis
427 in chili pepper stems (Figure 5d). In tomato stems, dsRNA treatments targeting Pc18476, Pc9358,
428 and Pc503811 effectively prevented necrosis and exhibited pathogen growth reductions of 18%,
429 34%, and 9%, respectively, relative to control.

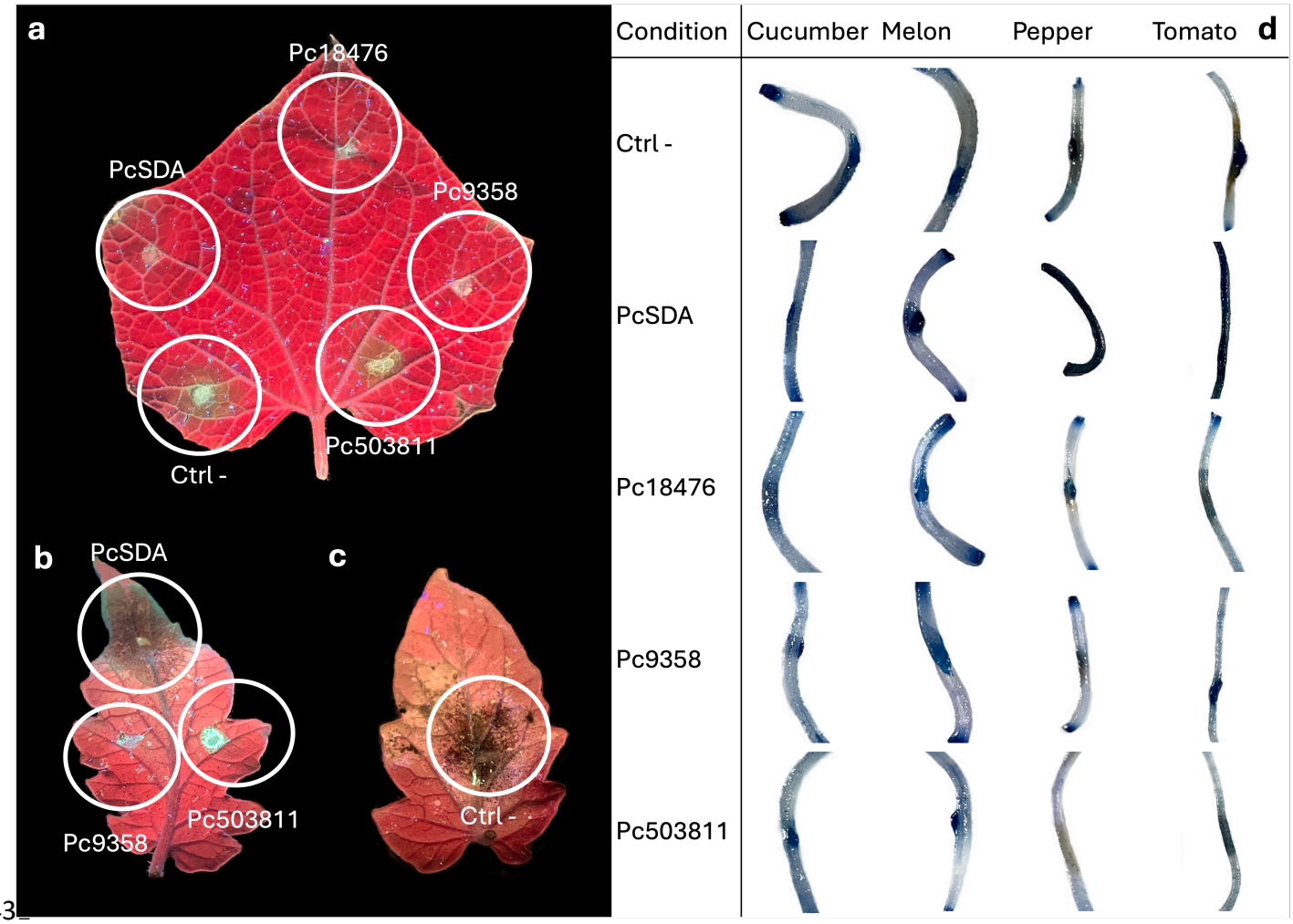

Figure 5: *P. capsici* gene silencing phenotypes. **a** Cucumber detached leaf inoculated with *P. capsici* treated with dsRNAs targeting PcSDA, Pc18476, Pc9358 and Pc503811 or control treated with dsRNA buffer without dsRNA production after 96hpi. **b** Tomato leaf inoculated with dsRNA treated *P. capsici* after 72hpi. **c** Tomato leaf inoculated with control *P. capsici* after 72hpi. **d** Trypan blue stained stems of cucumber, melon, tomato and chili pepper plantlets inoculated with control or dsRNA treated *P. capsici* after 96hpi.

3.6 Co-expression Analysis Uncovers Distinct Transcriptional Modules

The co-expression analysis of *P. capsici* during infection of cucumber, melon, chili pepper, and tomato revealed 10 distinct gene clusters with host-specific expression patterns and functional enrichments that together illuminate the adaptive strategies of the pathogen. For instance, the major

443 cluster 1 (1,999 genes) exhibits low expression in cucumber but is strongly induced in melon,
444 tomato, and chili pepper; it is enriched in processes such as ubiquitin-dependent protein
445 catabolism, vesicle-mediated transport and protein complex assembly. These functions, along with
446 pathways like propanoate and fatty acid metabolism as well as secretion components, suggest that
447 in hosts other than cucumber, the pathogen deploys rapid protein turnover and secretion
448 mechanisms to modulate its virulence arsenal effectively (Figure 5).
449
450 In contrast, cluster 2 (1,096 genes) is mostly active in cucumber, with intermediate levels in melon
451 and tomato and low expression in chili pepper. The enrichment of translation and nitrogen
452 metabolism within this cluster implies a heightened emphasis on protein synthesis and energy
453 acquisition during the more tolerant, delayed infection observed in cucumber. Complementing
454 these findings, a cluster 3 (832 genes) is specifically upregulated in chili pepper and shows strong
455 enrichment for central metabolic pathways including the tricarboxylic acid cycle, oxidative
456 phosphorylation, and carbohydrate transport which may reflect an attempt by *P. capsici* to
457 overcome the robust defense responses characteristic of this partially resistant host.
458
459 A distinct transcriptional signature is observed during tomato infection, where cluster 4 of 984
460 genes is predominantly induced. The overrepresentation of genes involved in protein amino acid
461 phosphorylation, the ubiquitin cycle, and microtubule-based movement in this group suggests that
462 rapid cytoskeletal reorganization and signal transduction are critical for the early, aggressive
463 colonization that leads to swift necrosis in tomato. Meanwhile, cluster 5 with 902 genes, highly
464 expressed in cucumber with intermediate levels in melon and chili pepper but low in tomato, is
465 enriched in pathways related to redox homeostasis, heme and pantothenate biosynthesis, and
466 glycolipid metabolism. This profile indicates that in cucumber, the pathogen may be fine-tuning
467 its lipid biosynthetic and redox-balancing processes to support a more prolonged infection.
468
469 Further complexity is added by cluster 6 of 741 genes that is upregulated in cucumber, melon, and
470 chili pepper but repressed in tomato; its enrichment in rRNA processing, ribosome biogenesis,
471 transcription, and tRNA processing underscores the importance of enhancing the pathogen's
472 translational machinery in hosts where colonization occurs over an extended period. Cluster 7 (603
473 genes) with moderate expression in cucumber and high expression in melon andchili pepper albeit

with fewer significant GO terms shows modulation of pathways such as porphyrin and pyrimidine metabolism, hinting at a role in fine-tuning gene expression and nuclear-cytoplasmic transport in response to host defenses.

Notably, a large set of 967 genes in cluster 8 is highly expressed in cucumber, melon, and tomato but is downregulated in chili pepper. This group is enriched for processes involved in cell communication, protein phosphorylation, phospholipid transport, and carbohydrate metabolism, along with nucleotide sugar and sphingoglycolipid metabolism. Such enrichments may reflect the active remodeling of membranes and signaling networks to optimize effector secretion and host interaction in the more susceptible hosts. In addition, cluster 9 comprising 577 genes (upregulated in cucumber, chili pepper, and tomato with low expression in melon) is enriched in pathways including mismatch repair, defense response, glycolysis, cell wall modification, and pathogenesis, suggesting these genes contribute to both virulence and the counteraction of host immune defenses (Figure 5).

Finally, a smaller, melon-specific cluster 10 of 381 genes, despite yielding no robust enrichments, likely represents a specialized set of factors that enable *P. capsici* to tailor its infection strategy to the unique metabolic or immune landscape of melon. Collectively, these integrated expression profiles illustrate how *P. capsici* differentially orchestrates metabolic, signaling, and structural processes to adapt to the distinct challenges and opportunities presented by each host.

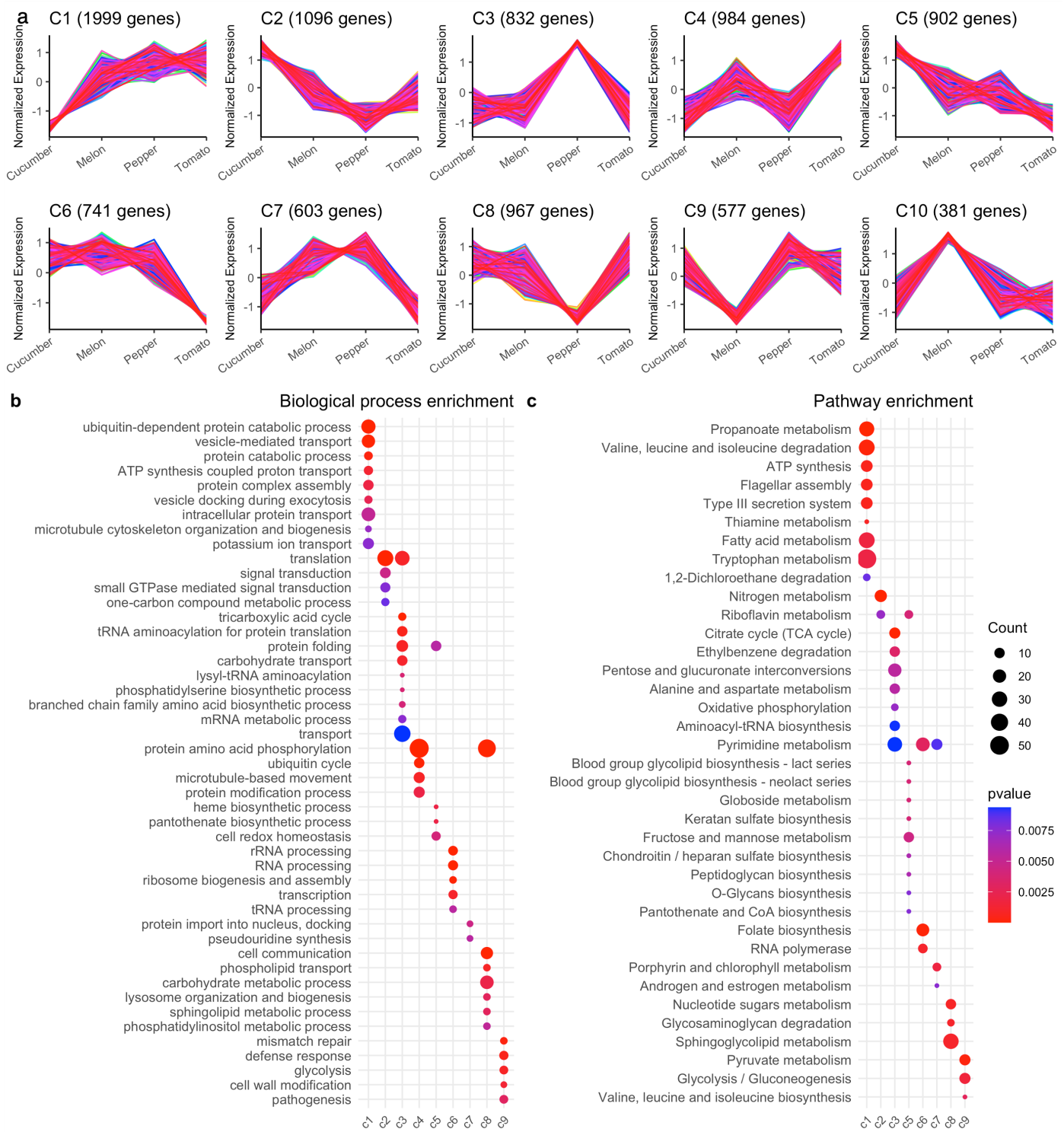

Figure 6: Clustering of co-expressed genes based on their expression profiles across infected host. **a** Each panel represents a cluster (C1–C10) with the number of genes indicated in parentheses. **b** Biological process and **c** KEGG Pathway enrichment of *P. capsici* clustered genes.

4 Discussion

4.1 Host-Specific Susceptibility and Pathogen Adaptation

Phytophthora capsici is a highly adaptable oomycete pathogen with a broad host range that includes economically important species from multiple plant families, notably Solanaceae and Cucurbitaceae. This wide host range is facilitated by its capacity to infect both root and aerial tissues, employ diverse infection strategies, and rapidly evolve virulence traits. However, the extent and nature of susceptibility vary markedly among host species, influenced by both preformed defenses and inducible immune responses (Quesada-Ocampo et al., 2023). Our study demonstrates that host susceptibility to *P. capsici* is not a uniform phenomenon but is distinctly modulated by host species. In tomato plants, a Solanaceous host, necrosis is visible as early as 12 hours post-inoculation for some individuals with a population median onset of 27 hpi, suggesting rapid cell death, which admits pathogen further colonization (Singh and Upadhyay, 2014). In contrast, cucurbitaceous hosts (cucumber and melon) exhibit delayed necrosis (first symptoms at 36–48 hpi with medians ranging from 54 to 102 hpi), yet these hosts support extensive intracellular colonization. This combination of delayed cell death and significant intracellular proliferation may reflect a more tolerant interaction. As defined in plant pathology, tolerance refers to a plant's ability to endure the presence of a pathogen without suffering significant loss in yield or quality, even though the pathogen may still infect and reproduce within the plant (Pagán and García-Arenal, 2018).

Our *Phytophthora* propagation findings in cucumber and melon align with previous studies that have documented a prolonged biotrophic phase in certain *Phytophthora* interactions. For example, in *P. infestans* infections of potato, a delayed necrotic induction is associated with sustained colonization that allows the pathogen to build up a critical biomass before a switch to necrotrophy (Lee and Rose, 2010; Schmelzer et al., 1995). In our system, the extensive vascular colonization observed in cucumber and melon via multiphoton microscopy suggests that these hosts may provide a relatively permissive environment that limits early defense activation. The result is a biotrophic scenario where *P. capsici* can establish a systemic infection while minimizing the rapid release of damage-associated molecular patterns (DAMPs) that typically trigger strong immune responses (Hernández-Chávez et al., 2017). Conversely, chili pepper (CM334), which has been

529 previously characterized as partially resistant (López-Martínez et al., 2011), shows delayed
530 necrosis coupled with an absence of intracellular colonization. We indeed observe that *P. capsici*
531 was unable to penetrate chili pepper plants. This indicates that in resistant hosts, preformed or
532 induced defenses such as reinforced cell walls and rapid antimicrobial signaling effectively restrict
533 pathogen entry and subsequent proliferation.
534 Recent transcriptomic studies have documented similar patterns. For instance (Maillot et al., 2022)
535 compared the transcriptomes of *P. capsici* infecting partially resistant CM334 chili pepper with
536 those infecting susceptible cultivars and found that in resistant tissues, the proliferation of
537 pathogen was blocked early by rapid defense signaling. In contrast, in susceptible tissues, the
538 pathogen showed the capacity to change the transcriptomic programming of the host responses to
539 delay necrosis and establish more robust colonization. Our findings extend these observations to
540 cucurbits, suggesting that the apparent tolerance in cucumber and melon could allow pathogen
541 proliferation by a more extended period for nutrient use and colonization.

542 **4.2 Unique Aspects of Crown Infection and Broader Implications**

543 A novel focus of our study is the infection initiation at the stem base and root crown rather than in
544 foliar tissues. Most studies on *Phytophthora* were focused on leaf infections (Chen et al., 2018; Li
545 et al., 2020; Zhu et al., 2016). However, pathogens such as *P. capsici* are transmitted by soil and
546 naturally target the crown region where roots and stem bases interface with the soil environment.
547 By examining these infection areas, we have uncovered critical insights into the early stages of
548 pathogen establishment. The crown region represents a crucial area with physical barriers and
549 localized immune responses that determine the success of infection (Bostock et al., 2014; Piccini
550 et al., 2019). In fact, results here exposed that *P. capsici* can establish extensive intracellular
551 colonization in the crown of cucurbitaceous hosts without triggering rapid necrosis, suggesting
552 that these tissues may offer a relatively protected niche that permits sustained pathogen growth
553 and eventual systemic colonization.
554
555 Understanding the dynamics of crown infection is particularly important for developing targeted
556 disease management strategies. In the case of cucurbits, in which the colonization is prolonged
557 due to delayed necrosis, then early detection and intervention strategies could focus on these
558 hidden infection sites before symptom development. From a theoretical perspective, breeding

559 programs that focus on enhancing crown resistance whether by reinforcing cell wall integrity or
560 amplifying localized immune responses could represent a promising avenue for achieving durable
561 resistance against *P. capsici* (Park et al., 2022). Additionally, differences in infection dynamics
562 between leaf and crown tissues may have broader implications for crop management strategies,
563 potentially influencing approaches to fungicide application and cultural practices. While these
564 concepts align with current understandings of plant defense mechanisms, further research would
565 be required to validate their practical effectiveness in disease control.
566
567 **4.3 Metabolic Reprogramming and Nutrient Acquisition**
568 The ability of *P. capsici* to reconfigure its metabolic networks in response to host-specific
569 conditions emerged as another central theme of our work. In tomato, the upregulation of glycolytic
570 and fatty acid metabolism pathways suggests a rapid mobilization of energy and biosynthetic
571 precursors to fuel aggressive colonization, a scenario commonly observed in necrotrophic
572 interactions (Kwaik and Bumann, 2015; Petrasch et al., 2019; Williams and Lorenz, 2020). In
573 cucurbits, however, our transcriptomic data revealed a pronounced enrichment of pathways related
574 to carbohydrate metabolism, galactose utilization, and glycerolipid metabolism. These alterations
575 may allow *P. capsici* to exploit the nutrient-rich vascular environment of cucumber and melon,
576 thereby supporting extensive intracellular colonization without triggering immediate cell death.
577 Such a strategy resembles the concept of "stealth colonization" wherein the pathogen minimizes
578 damage to host tissues to secure a longer-term nutritional niche (Petrasch et al., 2019; Williams
579 and Lorenz, 2020).
580
581 In chili pepper, (CM334, a genotype known to be partially resistant) the induction of metabolic
582 pathways associated with cell wall modification and nitrogen compound metabolism might reflect
583 adaptive responses to overcome the host's defensive mechanisms. It is probable that *P. capsici*
584 attempts to modify its own membranes and metabolic outputs to adapt better to a nutrient-scarce,
585 hostile environment imposed by robust host immunity. Such reprogramming may help to adapt to
586 a hostile microenvironment (Luo et al., 2021). This metabolic flexibility is emerging as a key
587 determinant of pathogen virulence and host adaptation, as also observed in other oomycetes (Ah-
588 Fong et al., 2017). The divergent metabolic signatures among hosts underscore the plasticity of *P.*
589 *capsici* physiology and its capacity to fine-tune nutrient acquisition strategies based on host-

590 derived signals. This versatility in metabolic reprogramming has been documented in other soil-
591 borne pathogens and is increasingly recognized as a key determinant of virulence and host
592 adaptation (Petrasch et al., 2019).
593
594 **4.4 Effector Dynamics and Host-Specific Virulence**
595 Effector proteins are key molecular tools employed by several pathogens to manipulate host
596 immunity and promote colonization. Oomycete effectors are broadly categorized into cytoplasmic
597 effectors and apoplastic effectors, depending on their localization and function (Bozkurt et al.,
598 2011). Our transcriptomic analysis revealed that *P. capsici* effector expression is tightly regulated
599 in a host-dependent manner. Among effector proteins, RxLR effectors are of particular interest for
600 their ability to translocate into host cells and suppress immune responses by targeting host
601 signaling pathways (Wang et al., 2023; Whisson et al., 2007). Our data show that while many
602 RxLR effectors are repressed, a subset is induced selectively depending on the host species. For
603 instance, homologs of PcAvh328 (Pc123179, Pc128001, and Pc552887), which have been shown
604 to interfere with host defense signaling, displayed differential expression patterns, with at least one
605 homolog being induced in chili pepper. Such induction in a typically resistant host may represent
606 a targeted effort by the pathogen to counteract strong basal defenses. Two previously
607 uncharacterized RxLR effectors (Pc503811 and Pc18476) were selected for functional analysis
608 using dsRNA-mediated silencing. Pc503811, induced specifically during infection in chili pepper
609 and tomato, and Pc18476, expressed in cucumber, melon, and tomato infections, displayed distinct
610 host-dependent roles. Silencing of Pc503811 resulted in a modest (18%) pathogen growth
611 reduction on detached cucumber leaves, whereas a substantial 76% growth reduction was observed
612 on detached tomato leaves compared to control treatments. During stem infections of cucumber
613 plantlets, silencing Pc503811 had no significant impact on pathogen growth. However, in melon
614 stems, although pathogen growth remained comparable to control, necrosis development was
615 prevented. Remarkably, in chili pepper stems, pathogen growth was notably reduced, and in tomato
616 stems, both pathogen growth reduction and necrosis prevention were observed. These results
617 suggest that Pc503811 function may be particularly relevant in interactions with solanaceous hosts.
618 The effector Pc18476, induced in all susceptible hosts, also showed host- and tissue-dependent
619 effects when silenced via dsRNA. On detached cucumber leaves, Pc18476 dsRNA treatment
620 resulted in a substantial 78% reduction in pathogen growth; however, this treatment had no

621 detectable effect on pathogen growth during infections of cucumber plantlet stems. In melon stems,
622 the pathogen growth was similar to controls, yet necrosis development was prevented by the
623 dsRNA treatment. In chili pepper stems, pathogen growth was reduced by 54%, whereas in tomato
624 stems, growth was modestly reduced by 18%, but importantly, necrosis was completely prevented.
625
626 PcAvh16 homologs (Pc14944, Pc14948, and Pc533084), implicated in suppressing programmed
627 cell death (Wang et al., 2011), are differentially regulated, suggesting that *P. capsici* tailors its
628 effector deployment to prolong its biotrophic phase, particularly in hosts with rapid necrotic
629 responses like tomato. In contrast, the consistent downregulation of effectors such as PcAvh166
630 across hosts may indicate roles confined to early infection events or environmental conditions not
631 captured at our 24 hpi sampling. Moreover, our observations on elicitins (INF1 and INF2B) and
632 Nep1-like proteins (NLPs) underscore the complexity of effector regulation. Canonical elicitins
633 are well known from *P. infestans* to induce hypersensitive responses (Derevnina et al., 2016; Du
634 et al., 2017; Huitema et al., 2005); their repression in cucurbits could be interpreted as a deliberate
635 suppression to avoid triggering host defenses prematurely. In contrast, the unique induction of
636 PcNLP14 in chili pepper may represent a specialized mechanism to manipulate host cell death
637 pathways and modulate immune responses (Chen et al., 2018).
638
639 The NLP effector Pc9358, specifically induced during infections of chili pepper, exhibited host-
640 and tissue-dependent phenotypes when silenced by dsRNA. On detached cucumber leaves, Pc9358
641 silencing caused a 65% reduction in pathogen growth, although no effect was observed on
642 cucumber plantlet stems. In melon stems, pathogen growth was unaffected by the dsRNA
643 treatment, but the induction of necrosis was completely prevented. In chili pepper and tomato
644 stems, Pc9358 silencing reduced pathogen growth by 32% and 34%, respectively, and prevented
645 necrosis development in both hosts. Interestingly, this was the only effector silencing treatment
646 that successfully prevented necrosis in chili pepper stems.
647
648 We also selected Pc533030, encoding the conserved cell-cycle regulator SDA1, as a control for
649 evaluating the efficacy of dsRNA treatments on pathogen growth. This gene was non-differentially
650 expressed in our transcriptomic datasets but was previously shown to be essential for sporangial
651 morphology, mycelial growth, and virulence during susceptible chili pepper leaf infections (Zhu

652 et al., 2016). Treatment of *P. capsici* with PcSDA1 dsRNA resulted in a 76% reduction of pathogen
653 growth on cucumber detached leaves; however, pathogen growth unexpectedly increased by 10%
654 in tomato leaves. In plantlet stems, PcSDA1 dsRNA treatment caused severe and aggressive
655 necrosis in chili pepper and tomato, surpassing control infections and leading to complete tissue
656 necrosis. No changes were observed in cucumber stems, whereas necrosis was prevented in melon
657 stems.
658
659 The growth reduction observed in cucumber leaves is consistent with previous findings that SDA1
660 is critical for hyphal development and virulence. However, the increased growth in tomato leaves
661 and the exacerbated necrosis in tomato and chili stems are unexpected and may reflect a
662 compensatory or stress-induced hypervirulence response when the cell cycle is disrupted
663 (Goncheva et al., 2019). This raises the possibility that interference with essential cellular functions
664 in *P. capsici* might dysregulate effector release or stress signaling, enhancing host tissue damage
665 in some contexts (Goncheva et al., 2019). Conversely, the absence of necrosis in melon stems
666 might indicate a differential host response to weakened or developmentally impaired pathogen
667 tissue. Altogether, these findings illustrate the complexity of targeting conserved genes and
668 highlight that silencing even core regulators like SDA1 can lead to variable outcomes depending
669 on the infection environment, host genotype, or tissue type.
670
671 Recent reviews have described that the spatial and temporal regulation of effectors is crucial for
672 pathogen success (Wang et al., 2023). Our study extends these findings by demonstrating that the
673 expression profiles of effectors are not only host-specific but may also be influenced by the
674 infection niche in our case, the crown region comprising the stem base and roots. This localized
675 deployment of effectors may reflect an adaptation to the unique defense barriers and nutrient
676 landscapes encountered at the soil-plant interface, where rapid colonization of vascular tissues can
677 be pivotal for systemic infection.
678
679 **5 Conclusions**
680 We found that *Phytophthora capsici* developed an adaptive strategy to colonize diverse plant
681 species. In tomato, rapid necrosis limits pathogen spread, yet aggressive metabolic reprogramming
682 supports early infection. On the other hand, the slow necrosis induction in cucumber and melon

683 coupled with extensive intercellular colonization, points to a tolerant interaction that may facilitate
684 prolonged pathogen proliferation. In partially resistant chili pepper CM334, robust defense
685 mechanisms inhibit intercellular colonization despite transcriptional changes in the pathogen. Our
686 comprehensive pathogen-centered transcriptomic analysis reveals that differential effector
687 deployment, metabolic reprogramming, and nutrient acquisition strategies are key components of
688 *P. capsici* adaptive virulence. This study highlights the value of examining the pathogen's
689 transcriptional dynamics, an approach often overlooked in favor of host-focused analyses. By
690 focusing on crown infections, this work expands our understanding of soil-borne infection
691 dynamics, a perspective that has been underrepresented in studies that predominantly target foliar
692 diseases.
693
694 **Declaration of competing interest**
695 The authors declare no conflict of interest.
696
697 **Data availability**
698 The raw reads generated during the current study are publicly available at NCBI under the
699 PRJNA1207595 accession number. Materials are available from the corresponding author upon
700 reasonable request.
701
702 **Acknowledgments**
703 This work forms part of the requirements for P.V.M. to obtain a Doctoral degree from the Posgrado
704 en Ciencias Biológicas program at Universidad Nacional Autónoma de México (UNAM). P.V.M.
705 receives a doctoral fellowship from Secretaria de Ciencia, Humanidades, Tecnología e Innovación
706 (SECIHTI). F.U.R.R. receives a posdoctoral fellowship from "Estancias Posdoctorales por México
707 2022" supported by SECIHTI. Funding was provided by PAPIIT-DGAPA-UNAM (project
708 IN218024) and SECIHTI (project A1-S-34759) to JV-A.
709
710 **References**
711 Abu-Jamous, B. & Kelly, S. (2018) Clust: automatic extraction of optimal co-expressed gene
712 clusters from gene expression data. *Genome Biology*, 19, 172.
713 https://doi.org/10.1186/s13059-018-1536-8.

714 Ah-Fong, A.M.V., Boyd, A.M., Matson, M.E.H. & Judelson, H.S. (2021) A Cas12a-based gene
715 editing system for Phytophthora infestans reveals monoallelic expression of an elicitor.
716 *Molecular Plant Pathology*, 22, 737–752. https://doi.org/10.1111/mpp.13051.

717 Ah-Fong, A.M.V., Kim, K.S. & Judelson, H.S. (2017) RNA-seq of life stages of the oomycete
718 Phytophthora infestans reveals dynamic changes in metabolic, signal transduction, and
719 pathogenesis genes and a major role for calcium signaling in development. *BMC*
720 *Genomics*, 18, 198. https://doi.org/10.1186/s12864-017-3585-x.

721 Bostock, R.M., Pye, M.F. & Roubtsova, T.V. (2014) Predisposition in Plant Disease: Exploiting the
722 Nexus in Abiotic and Biotic Stress Perception and Response. *Annual Review of*
723 *Phytopathology*, 52, 517–549. https://doi.org/10.1146/annurev-phyto-081211-172902.

724 Bozkurt, T.O., Schornack, S., Win, J., Shindo, T., Ilyas, M., Oliva, R., et al. (2011) Phytophthora
725 infestans effector AVRblb2 prevents secretion of a plant immune protease at the
726 haustorial interface. *Proceedings of the National Academy of Sciences*, 108, 20832–
727 20837. https://doi.org/10.1073/pnas.1112708109.

728 Bray, N.L., Pimentel, H., Melsted, P. & Pachter, L. (2016) Near-optimal probabilistic RNA-seq
729 quantification. *Nature Biotechnology*, 34, 525–527. https://doi.org/10.1038/nbt.3519.

730 Chen, X., Li, Y., Xing, Y., Xu, J. & Tong, Y. (2015) Cloning, transcriptional profiles and roles of
731 *Phytophthora capsici* CRN-encoding genes in the interaction with host plants. *Acta*
732 *Phytopathologica Sinica*, 45, 384–394.
733 https://doi.org/10.13926/j.cnki.apps.2015.04.007.

734 Chen, X.-R., Huang, S.-X., Zhang, Y., Sheng, G.-L., Li, Y.-P. & Zhu, F. (2018) Identification and
735 functional analysis of the NLP-encoding genes from the phytopathogenic oomycete
736 Phytophthora capsici. *Molecular genetics and genomics: MGG*, 293, 931–943.
737 https://doi.org/10.1007/s00438-018-1432-7.

738 Chen, X.-R., Xing, Y.-P., Li, Y.-P., Tong, Y.-H. & Xu, J.-Y. (2013) RNA-Seq Reveals Infection-Related
739 Gene Expression Changes in Phytophthora capsici. *PLOS ONE*, 8, e74588.
740 https://doi.org/10.1371/journal.pone.0074588.

741 Chepsergon, J., Motaung, T.E. & Moleleki, L.N. “Core” RxLR effectors in phytopathogenic
742 oomycetes: A promising way to breeding for durable resistance in plants? *Virulence*, 12,
743 1921–1935. https://doi.org/10.1080/21505594.2021.1948277.

744 Derevnina, L., Dagdas, Y.F., De la Concepcion, J.C., Bialas, A., Kellner, R., Petre, B., et al. (2016)
745 Nine things to know about elicitins. *New Phytologist*, 212, 888–895.
746 https://doi.org/10.1111/nph.14137.

747 Du, J., Guo, X., Chen, L., Xie, C. & Liu, J. (2017) Proteomic analysis of differentially expressed
748 proteins of Nicotiana benthamiana triggered by INF1 elicitin from Phytophthora

749 infestans. *Journal of General Plant Pathology*, 83, 66–77.
750 https://doi.org/10.1007/s10327-017-0699-6.

751 Fedkenheuer, K.E. (2016) Molecular Analysis of Oomycete Pathogens to Identify and Translate
752 Novel Resistance Mechanisms to Crops.

753 Feng, B.-Z., Zhu, X.-P., Fu, L., Lv, R.-F., Storey, D., Tooley, P., et al. (2014) Characterization of
754 necrosis-inducing NLP proteins in Phytophthora capsici. *BMC Plant Biology*, 14, 126.
755 https://doi.org/10.1186/1471-2229-14-126.

756 Goncheva, M.I., Flannagan, R.S., Sterling, B.E., Laakso, H.A., Friedrich, N.C., Kaiser, J.C., et al.
757 (2019) Stress-induced inactivation of the Staphylococcus aureus purine biosynthesis
758 repressor leads to hypervirulence. *Nature Communications*, 10, 775.
759 https://doi.org/10.1038/s41467-019-08724-x.

760 Grigoriev, I.V., Nikitin, R., Haridas, S., Kuo, A., Ohm, R., Otillar, R., et al. (2014) MycoCosm portal:
761 gearing up for 1000 fungal genomes. *Nucleic Acids Research*, 42, D699–D704.
762 https://doi.org/10.1093/nar/gkt1183.

763 Hausbeck, M.K. & Lamour, K.H. (2004) Phytophthora capsici on Vegetable Crops: Research
764 Progress and Management Challenges. *Plant Disease*, 88, 1292–1303.
765 https://doi.org/10.1094/PDIS.2004.88.12.1292.

766 Hernández-Chávez, M.J., Pérez-García, L.A., Niño-Vega, G.A. & Mora-Montes, H.M. (2017)
767 Fungal Strategies to Evade the Host Immune Recognition. *Journal of Fungi*, 3, 51.
768 https://doi.org/10.3390/jof3040051.

769 Huerta-Cepas, J., Szklarczyk, D., Heller, D., Hernández-Plaza, A., Forslund, S.K., Cook, H., et al.
770 (2019) eggNOG 5.0: a hierarchical, functionally and phylogenetically annotated
771 orthology resource based on 5090 organisms and 2502 viruses. *Nucleic Acids Research*,
772 47, D309–D314. https://doi.org/10.1093/nar/gky1085.

773 Huitema, E., Vleeshouwers, V.G.A.A., Cakir, C., Kamoun, S. & Govers, F. (2005) Differences in
774 Intensity and Specificity of Hypersensitive Response Induction in Nicotiana spp. by INF1,
775 INF2A, and INF2B of Phytophthora infestans. *Molecular Plant-Microbe Interactions®*, 18,
776 183–193. https://doi.org/10.1094/MPMI-18-0183.

777 Judelson, H.S. (2017) Metabolic Diversity and Novelties in the Oomycetes. *Annual Review of*
778 *Microbiology*, 71, 21–39. https://doi.org/10.1146/annurev-micro-090816-093609.

779 Jupe, J., Stam, R., Howden, A.J., Morris, J.A., Zhang, R., Hedley, P.E., et al. (2013) Phytophthora
780 capsici-tomato interaction features dramatic shifts in gene expression associated with a
781 hemi-biotrophic lifestyle. *Genome Biology*, 14, R63. https://doi.org/10.1186/gb-2013-
782 14-6-r63.

783 Knight, N.L. & Sutherland, M.W. (2016) Histopathological Assessment of Fusarium
784 pseudograminearum Colonization of Cereal Culms During Crown Rot Infections. *Plant*
785 *Disease*, 100, 252–259. https://doi.org/10.1094/PDIS-04-15-0476-RE.

786 Kwaik, Y.A. & Bumann, D. (2015) Host Delivery of Favorite Meals for Intracellular Pathogens.
787 *PLOS Pathogens*, 11, e1004866. https://doi.org/10.1371/journal.ppat.1004866.

788 Lamour, K.H., Mudge, J., Gobena, D., Hurtado-Gonzales, O.P., Schmutz, J., Kuo, A., et al. (2012a)
789 Genome sequencing and mapping reveal loss of heterozygosity as a mechanism for rapid
790 adaptation in the vegetable pathogen Phytophthora capsici. *Molecular plant-microbe*
791 *interactions: MPMI*, 25, 1350–1360. https://doi.org/10.1094/MPMI-02-12-0028-R.

792 Lamour, K.H., Stam, R., Jupe, J. & Huitema, E. (2012b) The oomycete broad-host-range pathogen
793 Phytophthora capsici. *Molecular Plant Pathology*, 13, 329–337.
794 https://doi.org/10.1111/j.1364-3703.2011.00754.x.

795 Lee, S.-J. & Rose, J.K.C. (2010) Mediation of the transition from biotrophy to necrotrophy in
796 hemibiotrophic plant pathogens by secreted effector proteins. *Plant Signaling &*
797 *Behavior*, 5, 769–772. https://doi.org/10.4161/psb.5.6.11778.

798 Lenarčič, T., Albert, I., Böhm, H., Hodnik, V., Pirc, K., Zavec, A.B., et al. (2017) Eudicot plant-
799 specific sphingolipids determine host selectivity of microbial NLP cytolysins. *Science*,
800 358, 1431–1434. https://doi.org/10.1126/science.aan6874.

801 Li, Q., Wang, J., Bai, T., Zhang, Ming, Jia, Y., Shen, D., et al. (2020) A Phytophthora capsici effector
802 suppresses plant immunity via interaction with EDS1. *Molecular Plant Pathology*, 21,
803 502–511. https://doi.org/10.1111/mpp.12912.

804 López-Martínez, N., Colinas-León, Ma.T., Peña-Valdivia, C.B., Salinas-Moreno, Y., Fuentes-
805 Montiel, P., Biesaga, M., et al. (2011) Alterations in peroxidase activity and
806 phenylpropanoid metabolism induced by Nacobbus aberrans Thorne and Allen, 1944 in
807 chilli (Capsicum annuum L.) CM334 resistant to Phytophthora capsici Leo. *Plant and Soil*,
808 338, 399–409. https://doi.org/10.1007/s11104-010-0553-5.

809 Love, M.I., Huber, W. & Anders, S. (2014) Moderated estimation of fold change and dispersion
810 for RNA-seq data with DESeq2. *Genome Biology*, 15, 550.
811 https://doi.org/10.1186/s13059-014-0550-8.

812 Luo, M., Sun, X., Qi, Y., Zhou, J., Wu, X. & Tian, Z. (2021) Phytophthora infestans RXLR effector
813 Pi04089 perturbs diverse defense-related genes to suppress host immunity. *BMC Plant*
814 *Biology*, 21, 582. https://doi.org/10.1186/s12870-021-03364-0.

815 Maillot, G., Szadkowski, E., Massire, A., Brunaud, V., Rigaill, G., Caromel, B., et al. (2022) Strive or
816 thrive: Trends in Phytophthora capsici gene expression in partially resistant pepper.
817 *Frontiers in Plant Science*, 13. https://doi.org/10.3389/fpls.2022.980587.

Pagán, I. & García-Arenal, F. (2018) Tolerance to Plant Pathogens: Theory and Experimental Evidence. *International Journal of Molecular Sciences*, 19, 810. https://doi.org/10.3390/ijms19030810.

Park, R.F., Boshoff, W.H.P., Cabral, A.L., Chong, J., Martinelli, J.A., McMullen, M.S., et al. (2022) Breeding oat for resistance to the crown rust pathogen Puccinia coronata f. sp. avenae: achievements and prospects. *Theoretical and Applied Genetics*, 135, 3709–3734. https://doi.org/10.1007/s00122-022-04121-z.

Petrasch, S., Silva, C.J., Mesquida-Pesci, S.D., Gallegos, K., Abeele, C. van den, Papin, V., et al. (2019) Infection Strategies Deployed by Botrytis cinerea, Fusarium acuminatum, and Rhizopus stolonifer as a Function of Tomato Fruit Ripening Stage. *Frontiers in Plant Science*, 10. https://doi.org/10.3389/fpls.2019.00223.

Piccini, C., Parrotta, L., Faleri, C., Romi, M., Del Duca, S. & Cai, G. (2019) Histomolecular responses in susceptible and resistant phenotypes of *Capsicum annuum* L. infected with *Phytophthora capsici*. *Scientia Horticulturae*, 244, 122–133. https://doi.org/10.1016/j.scienta.2018.09.051.

Pons-Hernández, J.L., Guerrero-Aguilar, B.Z., González-Chavira, M.M., González-Pérez, E., Villalobos-Reyes, S., Muñoz-Sánchez, C.I., et al. (2020) Phenotypic variability of Phytophthora capsici isolates in Guanajuato. *Revista mexicana de ciencias agrícolas*, 11, 1891–1901. https://doi.org/10.29312/remexca.v11i8.2618.

Quesada-Ocampo, L.M., Parada-Rojas, C.H., Hansen, Z., Vogel, G., Smart, C., Hausbeck, M.K., et al. (2023) Phytophthora capsici: Recent Progress on Fundamental Biology and Disease Management 100 Years After Its Description. *Annual Review of Phytopathology*, 61, 185–208. https://doi.org/10.1146/annurev-phyto-021622-103801.

Schmelzer, E., Naton, B., Freytag, S., Rouhara, I., Küster, B. & Hahlbrock, K. (1995) Infection-induced rapid cell death in plants: a means of efficient pathogen defense. *Canadian Journal of Botany*, 73, 426–434. https://doi.org/10.1139/b95-279.

Sevillano-Serrano, J., Larsen, J., Rojas-Rojas, F.U. & Vega-Arreguín, J.C. (2024) Increasing virulence and decreasing fungicide sensitivity in Phytophthora capsici after continuous metalaxyl-chlorothalonil exposure. *Journal of Plant Pathology*, 106, 1583–1590. https://doi.org/10.1007/s42161-024-01713-0.

Singh, V.K. & Upadhyay, R.S. (2014) Fusaric acid induced cell death and changes in oxidative metabolism of Solanum lycopersicum L. *Botanical Studies*, 55, 66. https://doi.org/10.1186/s40529-014-0066-2.

Sperschneider, J. & Dodds, P.N. (2022) EffectorP 3.0: Prediction of Apoplastic and Cytoplasmic Effectors in Fungi and Oomycetes. *Molecular Plant-Microbe Interactions®*, 35, 146–156. https://doi.org/10.1094/MPMI-08-21-0201-R.

854 Stam, R., Motion, G.B., Martinez-Heredia, V., Boevink, P.C. & Huitema, E. (2021) A Conserved
855 Oomycete CRN Effector Targets Tomato TCP14-2 to Enhance Virulence. *Molecular plant-*
856 *microbe interactions: MPMI*, 34, 309–318. https://doi.org/10.1094/MPMI-06-20-0172-R.

857 Stephens, A.E., Gardiner, D.M., White, R.G., Munn, A.L. & Manners, J.M. (2008) Phases of
858 Infection and Gene Expression of Fusarium graminearum During Crown Rot Disease of
859 Wheat. *Molecular Plant-Microbe Interactions®*, 21, 1571–1581.
860 https://doi.org/10.1094/MPMI-21-12-1571.

861 Tanja, S. (2023) Differential Gene Expression Analysis with Kallisto & DESeq2.

862 Teufel, F., Almagro Armenteros, J.J., Johansen, A.R., Gíslason, M.H., Pihl, S.I., Tsirigos, K.D., et al.
863 (2022) SignalP 6.0 predicts all five types of signal peptides using protein language
864 models. *Nature Biotechnology*, 40, 1023–1025. https://doi.org/10.1038/s41587-021-
865 01156-3.

866 Wang, Q., Han, C., Ferreira, A.O., Yu, X., Ye, W., Tripathy, S., et al. (2011) Transcriptional
867 Programming and Functional Interactions within the Phytophthora sojae RXLR Effector
868 Repertoire. *The Plant Cell*, 23, 2064–2086. https://doi.org/10.1105/tpc.111.086082.

869 Wang, S., McLellan, H., Boevink, P.C. & Birch, P.R.J. (2023) RxLR Effectors: Master Modulators,
870 Modifiers and Manipulators. *Molecular plant-microbe interactions: MPMI*, 36, 754–763.
871 https://doi.org/10.1094/MPMI-05-23-0054-CR.

872 Whisson, S.C., Boevink, P.C., Moleleki, L., Avrova, A.O., Morales, J.G., Gilroy, E.M., et al. (2007) A
873 translocation signal for delivery of oomycete effector proteins into host plant cells.
874 *Nature*, 450, 115–118. https://doi.org/10.1038/nature06203.

875 Williams, R.B. & Lorenz, M.C. (2020) Multiple Alternative Carbon Pathways Combine To Promote
876 Candida albicans Stress Resistance, Immune Interactions, and Virulence. *mBio*, 11,
877 10.1128/mbio.03070-19. https://doi.org/10.1128/mbio.03070-19.

878 Wu, T., Hu, E., Xu, S., Chen, M., Guo, P., Dai, Z., et al. (2021) clusterProfiler 4.0: A universal
879 enrichment tool for interpreting omics data. *The Innovation*, 2.
880 https://doi.org/10.1016/j.xinn.2021.100141.

881 Zhu, C., Yang, X., Lv, R., Li, Z., Ding, X., Tyler, B.M., et al. (2016) hytophthora capsici homologue
882 of the cell cycle regulator 1 is required for sporangial morphology, mycelial growth and
883 plant infection. *Molecular Plant Pathology*, 17, 369–387.
884 https://doi.org/10.1111/mpp.12285.

885 Zuluaga, A.P., Vega-Arreguín, J.C., Fei, Z., Ponnala, L., Lee, S.J., Matas, A.J., et al. (2016)
886 Transcriptional dynamics of Phytophthora infestans during sequential stages of
887 hemibiotrophic infection of tomato. *Molecular Plant Pathology*, 17, 29–41.
888 https://doi.org/10.1111/mpp.12263.